

Contribution from the Departments of Chemistry, University of Canterbury, Christchurch, New Zealand, and Stanford University, Stanford, California 94305

## Crystal and Molecular Structure of a Novel, High-Spin, Iron(II) "Picket Fence" Porphyrin Derivative. *catena*- $\{\mu$ -[*meso*-Tetrakis( $\alpha,\alpha,\alpha,\alpha$ -*o*-pivalamidophenyl)-porphinato-*N,N',N'',N'''*:O]-aquoiron(II)-tetrahydrothiophene}

G. B. JAMESON,<sup>1a</sup> WARD T. ROBINSON,<sup>\*1a</sup> JAMES P. COLLMAN,<sup>1b</sup> and THOMAS N. SORRELL<sup>1b</sup>

Received September 9, 1977

The crystal and molecular structure of the title compound has been determined using three-dimensional x-ray diffraction data ( $2\theta < 41^\circ$ ) collected by counter methods on an automatic diffractometer and refined using 2576 reflections having  $I > \sigma_I$  so that  $R = 0.116$  and  $R_w = 0.104$ . Crystal data: orthorhombic;  $P2_12_12_1$ ;  $a = 15.448$  (4),  $b = 26.481$  (6),  $c = 14.960$  (4) Å, for  $Z = 4$  and empirical formula  $\text{FeC}_{64}\text{N}_8\text{O}_4\text{H}_{64}\cdot\text{OH}_2\cdot\text{SC}_4\text{H}_8$ ;  $\rho_{\text{calcd}} = 1.27$ ,  $\rho_{\text{exptl}} = 1.25$  (1)  $\text{g cm}^{-3}$ . The crystal structure contains connected units of  $\text{Fe}(\text{TpivPP})$  with the iron atom of one unit coordinated to the pivalamide oxygen atom of another unit at a separation of 2.22 (1) Å. These infinite chains are separated by solvate molecules of tetrahydrothiophene. A water molecule is semicoordinated to the iron atom on the hindered side at a separation of 2.89 (2) Å. The iron atom is displaced 0.28 Å from the least-squares plane of the porphinato nitrogen atoms. The average  $\text{Fe}-\text{N}_{\text{porph}}$  separation is 2.068 (14) Å.

### Introduction

The stereochemistry of porphinato complexes is of continuing interest and the variation in stereochemistry as a function of metal center and axial ligands has been studied systematically.<sup>2</sup> The structures of iron and cobalt porphinato complexes have been of more immediate interest with regard to understanding the structure and function of the hemo-proteins.

The title compound was prepared as a result of attempts to obtain better quality crystals of  $[\text{Fe}(\text{TpivPP})(\text{THT})]\cdot 2(\text{THT})$ .<sup>3</sup> This latter complex, which coordinates dioxygen reversibly in the solid state, is a possible model for the oxygenated intermediate of cytochrome P450 camphor hydroxylase—an oxygen-binding hemoprotein.<sup>4</sup> Chang and Dolphin<sup>5</sup> have inferred that, for this stage, there is axial ligation of sulfur as a thiol species and not as a thiolate species. Thiolate axial ligation has been established for other intermediates in the catalytic cycle.<sup>6</sup> The structure of this iron-dioxygen complex is briefly described in footnote 15; the structure is only semiquantitative because the best diffraction data obtainable are extremely limited in quality and extent.

The title compound, polymeric  $[\text{Fe}(\text{TpivPP})(\text{OH}_2)]\cdot\text{THT}$ , has a number of novel features which are described in subsequent sections.

### Experimental Section

Tetrahydrothiophene (THT) was distilled from sodium under nitrogen; heptane was degassed by purging with pure nitrogen before use.  $[\text{Cr}(\text{acac})_2]_2$ <sup>7</sup> and  $\text{Fe}(\text{TpivPP})\text{Br}$ <sup>8</sup> were prepared by published procedures, and magnetic moments and gas evolution measurements were performed as previously described.<sup>8</sup> All operations were carried out in a Vacuum Atmospheres inert atmosphere box with a Model 40-A gas purifying system (<1 ppm oxygen). Analyses were performed by the microanalytical lab at Stanford University.

**Tris(tetrahydrothiophene)- $\alpha,\alpha,\alpha,\alpha$ -tetrapivalamidophenylporphyrinatoiron(II).** One hundred milligrams of  $\text{FeTpivPPBr}$  and 35 mg of  $[\text{Cr}(\text{acac})_2]_2$  were heated to boiling in 3 mL of THT for 5 min. Fifteen milliliters of heptane was added and the hot solution filtered by suction. After the addition of 20 mL of heptane, the solution was allowed to cool to room temperature overnight. The deep purple crystals were filtered, washed with heptane, and dried. Anal. Calcd for  $\text{C}_{76}\text{H}_{88}\text{N}_8\text{O}_4\text{FeS}_3$ : C, 68.7; H, 6.67; N, 8.43; Fe, 4.2; S, 7.23. Found: C, 68.7; H, 6.71; N, 8.48; Fe, 4.5; S, 7.14.

The magnetic moment of this complex is 5.0  $\mu_B$  (under argon). However, upon exposure to oxygen, the moment decreases to zero, indicating formation of the dioxygen adduct. Quantitative gas evolution measurements show that  $1.00 \pm 0.05$  equiv of  $\text{O}_2$  are bound per iron. Carbon monoxide reacts similarly, being bound irreversibly:  $\nu(\text{CO}) = 1970 \text{ cm}^{-1}$  (KBr),  $\mu = 0.0 \mu_B$ .

The Mössbauer spectrum of the  $\text{O}_2$  complex has been studied<sup>8</sup> and qualitatively appears very similar to the previous dioxygen adduct

$\text{Fe}(\text{TpivPP})(1\text{-Me-imid})(\text{O}_2)$ .<sup>8</sup> A more detailed discussion can be found in ref 9.

Occasionally, a second complex crystallizes from the solution prepared as described above. This material has the polymeric structure described below, although exact conditions for its formation are uncertain.

### Collection and Reduction of Intensity Data

Dark purple-black crystals of the title compound were prepared at Stanford University, sealed, and mailed to Canterbury University. Symmetry and systematic absences uniquely consistent with the orthorhombic space group  $P2_12_12_1$  were observed.<sup>10</sup> Most crystals, despite near-perfect cuboid habit, were twinned or very poorly mosaic. The cuboid crystal eventually chosen for data collection upon an Hilger and Watts four-circle, computer-controlled diffractometer had dimensions  $0.25 \times 0.25 \times 0.15 \text{ mm}^3$ . Zr-filtered  $\text{Mo K}\alpha$  x radiation was used. Crystal mosaicities for strong low-angle reflections, as determined by open counter  $\omega$  scans at a takeoff angle of  $3^\circ$ , ranged from 0.19 to  $0.35^\circ$ . Some peak profiles had a pronounced shoulder. Crystal orientation and unit cell dimensions at  $23^\circ \text{C}$  were obtained by least-squares refinement of the setting angles of 12 reflections accurately determined using a 5-mm diffracted beam collimator, the receiving aperture of which was 230 mm from the crystal. Dimensions thus obtained were  $a = 15.448$  (4),  $b = 26.415$  (6), and  $c = 14.960$  (4) Å. Here and elsewhere the estimated standard deviation (esd) in the least significant figures is quoted in parentheses and is conventionally derived from the inverse matrix during least-squares refinements. The calculated density for four formula units of  $\text{FeC}_{64}\text{N}_8\text{O}_4\text{H}_{64}\cdot\text{OH}_2\cdot\text{SC}_4\text{H}_8$  in the cell was  $1.27 \text{ g cm}^{-3}$ ; the observed density was  $1.25$  (1)  $\text{g cm}^{-3}$ . The linear absorption coefficient was  $3.45 \text{ cm}^{-1}$ , and since the maximum likely error due to neglect of absorption was less than 5%, absorption corrections were not applied. A total of 3674 unique reflections for which  $2\theta < 41^\circ$  were collected by the  $\theta$ - $2\theta$  scan technique. A symmetric scan range of  $1.40^\circ$  in  $2\theta$ , centered on the calculated peak position, comprised 70 steps each of 4-s duration. Stationary crystal, stationary counter background counts at each end of the scan were recorded for 70 s each. The intensities of three standard reflections, well-separated in reciprocal space and monitored every 50 reflections, each suffered a decrease of  $\sim 8\%$  over the period of data collection. The data were scaled and corrected for Lorentz and polarization effects. Details of the programs used and definitions of symbols are documented elsewhere.<sup>11</sup>

### Solution and Refinement of the Structure

Analysis of the three-dimensional Patterson synthesis yielded coordinates for the iron atom. This atom was given a temperature factor of  $B = 4.0$  and its position, together with an overall scale factor, was refined; the agreement factors  $R$  and  $R_w$  were 0.44 and 0.51 for 1522 reflections having  $I > 3\sigma_I$ . The orientation of the *meso*-tetraphenylporphinato species was deduced from a weighted  $F_o$  Fourier synthesis.<sup>12</sup> Successive cycles of Fourier syntheses and least-squares refinements established the positions in the asymmetric unit of the remaining nonhydrogen atoms of the  $\text{Fe}(\text{TpivPP})$  unit. The  $R$  factor was lowered to 0.18. At this stage a difference Fourier synthesis

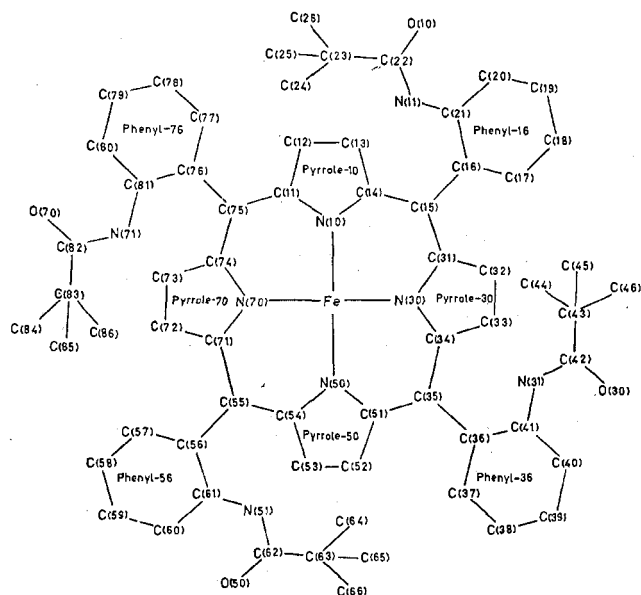


Figure 1. Atom and group labeling scheme for polymeric  $[\text{Fe}(\text{TpivPP})(\text{OH}_2)] \cdot \text{THT}$ .

revealed the position of the THT solvate molecule. Although subsequent least-squares refinements showed that the sulfur atom had anomalously high thermal motion, Fourier syntheses and the stereochemistry of the refined solvate model did indicate that the sulfur atom was not disordered among the five atom sites.

Further least-squares refinement led to  $R = 0.13$  and the subsequent difference Fourier synthesis again indicated electron density at  $\sim 2.9 \text{ \AA}$  from the iron atom. This was included in the model as an oxygen atom and the model refined so that  $R = 0.12$  and  $R_w = 0.14$ . Group constraints on pyrrole and *tert*-butyl groups were progressively released and selected atoms allowed an anisotropic model for thermal motion. Reflections having  $I > \sigma_I$  were used and for the final four cycles of least-squares refinement the model was described by 480 variable parameters split into two blocks of 354 parameters with the relative contents of each block changed between cycles. The thermal ellipsoid parameters of two atoms N(31) and C(84) became nonpositive definite on the first cycle. The appropriate  $\beta_H$  term was adjusted (by less than

one esd) so that the atom had physically meaningful thermal ellipsoid parameters, and these parameters were held constant for subsequent cycles. Refinements converged with agreement factors  $R$  and  $R_w$  of 0.116 and 0.104 for 2576 reflections having  $I > \sigma_I$ . A structure factor calculation in the enantiomorphic space group gave higher agreement factors; the original enantiomorph was taken as correct. The standard error in an observation of unit weight is 1.461. In the final two cycles the ratios of change in a parameter to its esd were all less than 0.75. A difference Fourier map calculated prior to the final four cycles was flat and featureless; the highest peak had  $0.39 \text{ e \AA}^{-3}$  compared to  $1.35 \text{ e \AA}^{-3}$  for the last located atom. There was little evidence for secondary extinction among strong low-angle reflections. Since the averaged values of the minimized function were independent of  $|F_o|$  and  $(\sin \theta)/\lambda$ , the weighting scheme ( $p = 0.074$ ) was judged satisfactory. A table of  $|F_o|$  and  $|F_c|$  for all data is contained in the supplementary material. There are no serious discrepancies between  $|F_o|$  and  $|F_c|$  with respect to  $\sigma_{|F_o|}$ . Final atomic parameters and root mean square amplitudes of thermal displacement are quoted in Tables I and II. The atom labeling scheme is illustrated in Figure 1.

### Description of the Structure

The crystal structure consists of infinite chains of Fe-(TpivPP) units, a pivalamide oxygen atom, O(30), of one unit is coordinated to the iron atom of another at a separation of  $2.22 (1) \text{ \AA}$ . Solvate molecules of tetrahydrothiophene occupy interstices in the crystal lattice. A water molecule is nestled among the pivalamide "pickets"  $2.90 (2) \text{ \AA}$  from the iron atom.

The coordination geometry about the iron center is approximately square pyramidal. The iron atom is displaced  $0.28 \text{ \AA}$  from the least-squares plane of the porphyrin nitrogen atoms toward the coordinated pivalamide oxygen atom, and  $0.33 \text{ \AA}$  from the least-squares plane of the 24-atom porphyrin skeleton. The porphyrin skeleton, therefore, has a value for the doming parameter<sup>2</sup> of  $0.05 \text{ \AA}$ .

Figure 2 is a stereodiagram of two linked units; crystal packing is illustrated in Figure 3. Bond distances and angles, together with the average value for a given class of distance or angle are contained in Tables III and IV. Inspection of these tables shows that, in the main, the structure is internally consistent.

Table V lists nonbonded contacts between Fe(TpivPP) units and solvate molecules. It can be seen that, despite the awkward

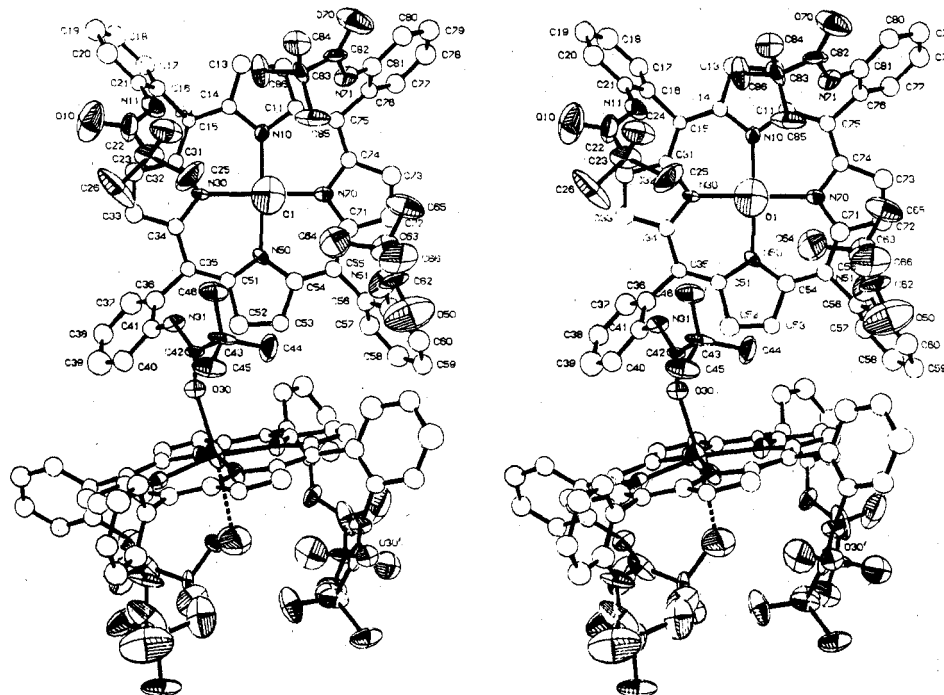


Figure 2. An ORTEP stereodiagram of two units of polymeric Fe(TpivPP). Thermal ellipsoids are drawn at the 40% probability level. The atom labeling system for both structures is also defined.

Table I. Final Atomic Parameters

(a) Individually Refined Atoms<sup>a,b</sup>

Atom	x	y	z	$\beta_{11}$	$\beta_{22}$	$\beta_{33}$	$\beta_{12}$	$\beta_{13}$	$\beta_{23}$
Fe	03337 (18)	-2077 (10)	13497 (19)	00536 (16)	00138 (4)	00639 (18)	00093 (9)	00283 (17)	00107 (9)
O(1)	1616 (14)	-2332 (8)	2689 (13)	0148 (16)	0044 (6)	0118 (15)	-0000 (8)	-0038 (14)	-0006 (7)
N(10)	-0495 (8)	-2112 (5)	2417 (9)	0027 (7)	0009 (2)	0052 (8)	0002 (4)	0004 (7)	0003 (4)
N(30)	0228 (8)	-2855 (5)	1220 (8)	0027 (6)	0013 (2)	0034 (7)	-0002 (4)	0016 (7)	0002 (4)
N(50)	1425 (9)	-2102 (6)	0534 (8)	0047 (8)	0013 (3)	0030 (8)	0002 (5)	0009 (7)	0009 (5)
N(70)	0684 (9)	-1352 (5)	1737 (9)	0027 (7)	0014 (3)	0037 (8)	-0002 (4)	0005 (7)	-0001 (4)
N(11)	-0133 (10)	-3697 (6)	3518 (12)	0048 (9)	0018 (3)	0070 (11)	-0016 (5)	0007 (9)	0001 (5)
O(10)	0257 (11)	-4509 (6)	3428 (18)	0084 (10)	0021 (3)	0313 (26)	-0008 (5)	0002 (17)	-0019 (8)
C(22)	0493 (22)	-4068 (10)	3549 (17)	0158 (28)	0013 (5)	0087 (17)	0019 (10)	0029 (20)	0006 (9)
C(23)	1426 (12)	-3934 (10)	3660 (18)	0008 (10)	0041 (7)	0086 (18)	0011 (7)	-0007 (12)	0019 (10)
C(24)	1648 (15)	-3869 (10)	4631 (16)	0062 (14)	0044 (7)	0081 (17)	0001 (8)	0012 (13)	0016 (9)
C(25)	1608 (17)	-3401 (10)	3245 (22)	0068 (16)	0035 (7)	0191 (30)	0026 (9)	0029 (18)	-0010 (12)
C(26)	1982 (18)	-4352 (12)	3253 (22)	0095 (20)	0059 (10)	0177 (31)	-0040 (12)	-0030 (20)	0072 (15)
N(31) <sup>c</sup>	3065 (8)	-3394 (6)	0259 (11)	0003	0021	0074	0003	0002	0007
O(30)	4310 (8)	-3190 (5)	-0420 (9)	0041 (7)	0018 (3)	0046 (8)	-0000 (4)	0008 (7)	-0001 (4)
C(42)	3852 (13)	-3226 (7)	0262 (15)	0039 (12)	0010 (4)	0069 (16)	-0008 (5)	0039 (12)	-0007 (6)
C(43)	4242 (12)	-3033 (9)	1156 (12)	0030 (10)	0037 (6)	0024 (11)	0000 (7)	0013 (9)	0013 (7)
C(44)	4432 (17)	-2460 (8)	1062 (14)	0133 (20)	0013 (4)	0077 (16)	0018 (8)	0023 (15)	-0002 (7)
C(45)	5127 (12)	-3320 (9)	1293 (15)	0028 (11)	0044 (6)	0069 (14)	-0011 (7)	0002 (12)	0002 (8)
C(46)	3638 (15)	-3173 (9)	1929 (13)	0072 (14)	0034 (6)	0030 (12)	0000 (8)	0013 (11)	0002 (6)
N(51)	3232 (12)	-0927 (8)	1737 (13)	0062 (13)	0040 (5)	0056 (13)	0022 (6)	-0039 (10)	-0005 (7)
O(50)	4492 (19)	-0848 (11)	2211 (16)	0148 (21)	0094 (10)	0112 (17)	0013 (13)	-0004 (17)	-0048 (10)
C(62)	3714 (19)	-0955 (12)	2369 (21)	0070 (18)	0055 (9)	0094 (23)	0048 (11)	0052 (17)	0028 (13)
C(63)	3605 (17)	1199 (8)	3276 (14)	0120 (19)	0024 ( )	0049 (14)	0006 (8)	0013 (14)	-0021 (7)
C(64)	3288 (23)	1756 (10)	3076 (18)	0190 (28)	0029 (6)	0082 (20)	0003 (12)	0038	-0016 (9)
C(65)	2879 (16)	-0911 (11)	3752 (19)	0073 (16)	0048 (8)	0087 (19)	-0035 (9)	0012 (16)	-0001 (10)
C(66)	4439 (13)	-1239 (11)	3889 (20)	0019 (12)	0062 (9)	0135 (25)	0006 (8)	-0024 (14)	0002 (12)
N(71)	0061 (10)	-1412 (6)	4729 (10)	0070 (11)	0018 (3)	0025 (8)	0015 (5)	0001 (8)	-0015 (4)
O(70)	-0058 (13)	-1507 (7)	6240 (11)	0181 (18)	0040 (4)	0072 (11)	-0036 (7)	0054 (13)	-0014 (6)
C(82)	0231 (15)	-1687 (9)	5508 (14)	0064 (14)	0034 (5)	0046 (12)	0025 (8)	0039 (12)	0018 (7)
C(83)	0715 (13)	-2185 (7)	5465 (13)	0060 (12)	0008 (4)	0057 (14)	-0008 (6)	0010 (12)	0007 (6)
C(84) <sup>c</sup>	0819 (16)	-2379 (8)	6402 (11)	0122	0028	0007	0004	-0001	-0008
C(85)	1555 (16)	-2084 (11)	4979 (15)	0080 (15)	0044 (7)	0065 (15)	-0012 (10)	0044 (13)	-0010 (10)
C(86)	0106 (14)	-2540 (7)	4885 (13)	0095 (16)	0014 (4)	0060 (13)	-0002 (6)	-0047 (12)	0004 (6)
S	3704 (12)	-4773 (8)	132 (3)	0168 (14)	0085 (6)	102 (8)	0002 (8)	011 (4)	0051 (20)
C(1)	455 (4)	-4718 (15)	034 (3)	022 (5)	0041 (9)	010 (3)	0006 (19)	002 (3)	0038 (12)
C(2)	523 (2)	-4677 (17)	065 (4)	009 (3)	0049 (10)	019 (5)	0050 (14)	000 (3)	-0007 (17)
C(3)	532 (3)	-4773 (13)	166 (3)	015 (4)	0037 (7)	014 (3)	-0027 (14)	008 (3)	-0020 (12)
C(4)	463 (3)	-4699 (18)	210 (3)	009 (3)	0083 (15)	016 (3)	-0021 (18)	-000 (3)	-0035 (18)

Atom	x	y	z	B, Å <sup>2</sup>	Atom	x	y	z	B, Å <sup>2</sup>
C(15)	-0925 (9)	-3007 (6)	2330 (10)	2.1 (3)	C(33)	0336 (12)	-3663 (6)	0694 (11)	4.0 (4)
C(35)	1363 (10)	-2994 (6)	0071 (11)	2.8 (4)	C(34)	0658 (11)	-3155 (6)	0641 (11)	3.1 (4)
C(55)	1902 (11)	-1222 (6)	0662 (12)	3.4 (4)	C(51)	1686 (11)	-2512 (7)	0048 (12)	3.0 (4)
C(75)	-0379 (12)	-1217 (6)	2959 (11)	3.2 (4)	C(52)	2439 (12)	-2377 (7)	-0545 (13)	4.4 (5)
C(11)	-0750 (11)	-1703 (7)	2943 (11)	3.1 (4)	C(53)	2566 (11)	-1869 (7)	-0351 (11)	3.3 (4)
C(12)	-1443 (11)	-1853 (6)	3494 (12)	3.8 (4)	C(54)	1943 (12)	-1695 (7)	0311 (12)	3.7 (4)
C(13)	-1635 (12)	-2364 (7)	3370 (12)	4.0 (4)	C(71)	1314 (12)	-1052 (7)	1321 (14)	4.4 (4)
C(14)	-1013 (10)	-2514 (7)	2680 (11)	2.7 (4)	C(72)	1300 (12)	-0544 (7)	1702 (13)	4.7 (5)
C(31)	-0349 (11)	-3159 (6)	1644 (10)	2.7 (3)	C(73)	0680 (12)	-0542 (7)	2357 (12)	4.4 (4)
C(32)	-0278 (11)	-3676 (6)	1355 (12)	3.9 (4)	C(74)	0269 (12)	-1055 (5)	2387 (11)	3.2 (4)

(b) Derived Parameters for Atoms Constrained in Rigid Groups<sup>d,e</sup>

Atom	x	y	z	B, Å	Atom	x	y	z	B, Å <sup>2</sup>
C(16)	-144 (1)	-3415 (6)	278 (1)	3.1 (4)	C(56)	255 (1)	-0841 (6)	035 (1)	3.8 (4)
C(17)	-233 (1)	-3456 (5)	261 (1)	4.2 (4)	C(57)	249 (1)	-0647 (8)	-051 (1)	4.6 (5)
C(18)	-2803 (8)	-3846 (7)	300 (1)	5.6 (5)	C(58)	312 (1)	-0314 (7)	-082 (1)	5.5 (5)
C(19)	-240 (1)	-4194 (6)	355 (1)	4.7 (5)	C(59)	380 (1)	-0176 (6)	-027 (1)	4.5 (4)
C(20)	-151 (1)	-4153	372 (1)	4.8 (5)	C(60)	386 (1)	-0370 (8)	059 (1)	5.3 (5)
C(21)	-1037 (8)	-3763 (7)	333 (1)	2.9 (4)	C(61)	323 (1)	-0702 (7)	090 (1)	5.1 (5)
H(17)	-261 (2)	-3219 (7)	223 (1)	6.0	H(57)	202 (1)	-074 (1)	-089 (2)	6.0
H(18)	-3407 (8)	-387 (1)	288 (2)	7.0	H(58)	308 (2)	-081 (1)	-141 (1)	7.0
H(19)	-272 (2)	-4461 (9)	382 (2)	6.0	H(59)	423 (1)	+0051 (8)	-049 (2)	6.0
H(20)	-123 (2)	-4390 (7)	410 (1)	6.0	H(60)	433 (1)	-028 (1)	097 (2)	6.0
C(36)	171 (1)	-3387 (7)	-056 (1)	4.0 (4)	C(76)	-062 (2)	-0851 (7)	368 (1)	3.1 (4)
C(37)	1201 (9)	-3563 (8)	-126 (1)	5.5 (5)	C(77)	-105 (1)	-0401 (6)	3470 (9)	4.3 (4)
C(38)	155 (1)	-3888 (6)	-190 (1)	4.7 (5)	C(78)	-130 (1)	-0072 (6)	415 (1)	5.0 (5)
C(39)	241 (1)	-4036 (7)	-184 (1)	6.7 (6)	C(79)	-112 (2)	-0193 (7)	504 (1)	4.9 (5)
C(40)	2927 (9)	-3859 (8)	-114 (1)	4.6 (5)	C(80)	-070 (1)	-0643 (6)	5245 (8)	4.3 (4)
C(41)	258 (1)	-3535 (6)	-050 (1)	3.7 (4)	C(81)	-045 (1)	-0972 (6)	457 (1)	4.1 (4)
H(37)	061 (1)	-346 (1)	-130 (2)	7.0	H(77)	-117 (1)	-0318 (9)	286 (1)	6.0
H(38)	120 (2)	-4008 (9)	-238 (1)	6.0	H(78)	-159 (2)	+0235 (8)	401 (2)	6.0
H(39)	265 (2)	-426 (1)	-228 (1)	7.0	H(79)	-129 (3)	+003 (1)	550 (1)	6.0
H(40)	352 (1)	-396 (1)	-110 (2)	6.0	H(80)	-058 (2)	-0726 (9)	5851 (9)	6.0

Table I (Continued)

(c) Rigid Group Parameters<sup>f</sup>

Group	x	y	z	$\varphi$	$\sigma$	$\rho$
Phenyl-16	-1920 (5)	-3805 (3)	3165 (5)	1.956 (8)	2.674 (7)	0.486 (7)
Phenyl-36	2064 (6)	-3711 (3)	-1202 (6)	1.536 (8)	2.652 (7)	-0.891 (8)
Phenyl-56	3175 (6)	-0508 (3)	0040 (6)	0.836 (8)	-2.799 (7)	1.197 (8)
Phenyl-76	-0872 (4)	-0522 (3)	4357 (6)	2.590 (10)	2.395 (6)	1.661 (10)

<sup>a</sup> Positional and anisotropic thermal parameters generated by placing 0. prior to the first digit. <sup>b</sup> The form of the anisotropic thermal ellipsoid is  $\exp[\beta_{11}h^2 + \beta_{22}k^2 + \beta_{33}l^2 + 2\beta_{13}hl + 2\beta_{23}kl]$ . <sup>c</sup> Thermal parameters not refined; see text. <sup>d</sup> Hydrogen atom H(17) attached to carbon atom C(17), etc. <sup>e</sup> Nonhydrogen atoms in rigid groups allowed individual temperature factors. <sup>f</sup> Group orientation defined by R. J. Doedens (Paper E3, International Summer School on Crystallography Computing, Ottawa, 1969); angles and radians.

Table II. Root-Mean-Square Components of Thermal Displacement along Principal Ellipsoidal Axes (Å)

Atom	RMS1	RMS2	RMS3	Atom	RMS1	RMS2	RMS3
Fe	0.188 (5)	0.190 (4)	0.338 (5)	N(51)	0.14 (4)	0.30 (3)	0.42 (3)
O(1)	0.32 (3)	0.40 (3)	0.45 (2)	O(50)	0.30 (3)	0.42 (3)	0.61 (3)
N(10)	0.17 (3)	0.19 (3)	0.25 (2)	C(62)	0.13 (6)	0.28 (4)	0.54 (4)
N(30)	0.12 (4)	0.22 (2)	0.23 (2)	C(63)	0.15 (5)	0.34 (3)	0.39 (3)
N(50)	0.14 (3)	0.22 (3)	0.26 (2)	C(64)	0.23 (4)	0.35 (4)	0.49 (4)
N(70)	0.17 (3)	0.21 (2)	0.23 (2)	C(65)	0.21 (4)	0.32 (3)	0.46 (3)
N(11)	0.16 (3)	0.28 (2)	0.31 (2)	C(66)	0.13 (5)	0.40 (4)	0.47 (3)
O(10)	0.25 (2)	0.33 (2)	0.60 (3)	N(71)	0.10 (4)	0.28 (2)	0.29 (2)
C(22)	0.19 (4)	0.30 (3)	0.45 (4)	O(70)	0.24 (3)	0.31 (2)	0.54 (3)
C(23)	0.06 (10)	0.28 (3)	0.41 (3)	C(82)	0.13 (5)	0.23 (3)	0.42 (3)
C(24)	0.25 (3)	0.30 (3)	0.41 (3)	C(83)	0.14 (5)	0.26 (3)	0.29 (3)
C(25)	0.19 (4)	0.40 (3)	0.47 (4)	C(84) <sup>a</sup>	0.07	0.32	0.39
C(26)	0.20 (5)	0.33 (4)	0.61 (4)	C(85)	0.18 (4)	0.34 (3)	0.42 (3)
N(31) <sup>a</sup>	0.06	0.26	0.31	C(86)	0.18 (4)	0.22 (3)	0.39 (3)
O(30)	0.20 (2)	0.244 (19)	0.257 (18)	S	0.432 (19)	0.540 (20)	1.09 (4)
C(42)	0.11 (6)	0.18 (4)	0.34 (3)	C(1)	0.23 (4)	0.45 (5)	0.52 (6)
C(43)	0.11 (5)	0.21 (3)	0.37 (3)	C(2)	0.18 (6)	0.47 (6)	0.50 (5)
C(44)	0.18 (4)	0.29 (3)	0.42 (3)	C(3)	0.27 (5)	0.32 (4)	0.54 (5)
C(45)	0.17 (4)	0.28 (3)	0.40 (3)	C(4)	0.30 (5)	0.39 (5)	0.58 (5)
C(46)	0.17 (4)	0.30 (3)	0.35 (3)				

<sup>a</sup> Thermal parameters not refined. See text.

Table III. Bond Distances<sup>a</sup>

Atoms	Distance	Average	Atoms	Distance	Average	Atoms	Distance	Average
Fe-N(10)	2.048 (13)		C(15)-C(14)	1.412 (21)		C(22)-C(23)	1.49 (3)	
Fe-N(30)	2.071 (13)		C(15)-C(31)	1.416 (20)		C(23)-C(24)	1.50 (3)	
Fe-N(50)	2.083 (13)		C(35)-C(34)	1.448 (21)		C(23)-C(25)	1.56 (3)	
Fe-N(70)	2.074 (14)	2.069 (15)	C(35)-C(51)	1.368 (22)		C(23)-C(26)	1.53 (3)	
Fe-O(1)	2.897 (19)		C(55)-C(54)	1.357 (22)		C(42)-C(43)	1.55 (3)	
Fe-O(30)'	2.221 (14)		C(55)-C(71)	1.413 (23)		C(43)-C(44)	1.55 (3)	
N(10)-C(11)	1.395 (19)		C(75)-C(74)	1.385 (21)		C(43)-C(45)	1.58 (3)	
N(10)-C(14)	1.386 (19)		C(75)-C(11)	1.404 (20)	1.400 (29)	C(43)-C(46)	1.53 (3)	
N(30)-C(31)	1.357 (18)		C(15)-C(16)	1.499		C(62)-C(63)	1.51 (4)	
N(30)-C(34)	1.348 (18)		C(35)-C(36)	1.508		C(63)-C(64)	1.58 (3)	
N(50)-C(51)	1.368 (21)		C(55)-C(56)	1.487		C(63)-C(65)	1.53 (3)	
N(50)-C(54)	1.378 (21)		C(75)-C(76)	1.495	1.497 (9)	C(63)-C(66)	1.58 (3)	
N(70)-C(71)	1.400 (21)		N(11)-C(21)	1.433		C(82)-C(83)	1.51 (3)	
N(70)-C(74)	1.402 (19)	1.380 (21)	N(31)-C(41)	1.416		C(83)-C(84)	1.50 (2)	
C(11)-C(12)	1.408 (22)		N(51)-C(61)	1.381		C(83)-C(85)	1.51 (3)	
C(13)-C(14)	1.464 (22)		N(71)-C(81)	1.424	1.414 (23)	C(83)-C(86)	1.59 (2)	1.54 (3)
C(31)-C(32)	1.437 (19)		N(11)-C(22)	1.38 (3)		S-C(1)	1.97 (5)	
C(33)-C(34)	1.432 (21)		N(31)-C(42)	1.29 (2)		S-C(4)	1.85 (5)	
C(51)-C(52)	1.505 (23)		N(51)-C(62)	1.21 (3)		C(1)-C(2)	1.15 (5)	
C(53)-C(54)	1.456 (22)		N(71)-C(82)	1.40 (3)	1.32 (9)	C(2)-C(3)	1.53 (5)	
C(71)-C(72)	1.459 (23)		C(22)-O(10)	1.234 (24)		C(3)-C(4)	1.27 (4)	
C(73)-C(74)	1.499 (22)	1.458 (33)	C(42)-O(30)	1.245 (19)				
C(12)-C(13)	1.394 (20)		C(62)-O(50)	1.257 (29)				
C(32)-C(33)	1.372 (22)		C(82)-O(70)	1.275 (22)	1.253 (18)			
C(52)-C(53)	1.388 (21)							
C(72)-C(73)	1.371 (23)	1.381 (12)						

<sup>a</sup> Esd's for bond parameters involving atoms constrained in rigid groups not calculated.

shape of the Fe(TpivPP) units, there are few contacts less than 3.45 Å. All such contacts involve pivalamide oxygen atoms which, with the exception of the coordinated atom, O(30), exhibit high thermal motion; irresolvable disorder for these atoms is inferred. The semicoordinated water molecular makes a number of close contacts with pivalamide methyl groups

(O(1)---C(25) 2.94 (3) Å, O(1)---C(64) 3.05 (4) Å); positional disorder for these atoms is again inferred. The packing constraints in linking two Fe(TpivPP) units are best appreciated by inspection of Figure 2. The Fe-O(30)' vector is canted 6.7° to the normal to the porphyrato plane and the Fe-O(30)'-C(42)' angle (160 (1)°) is considerably more

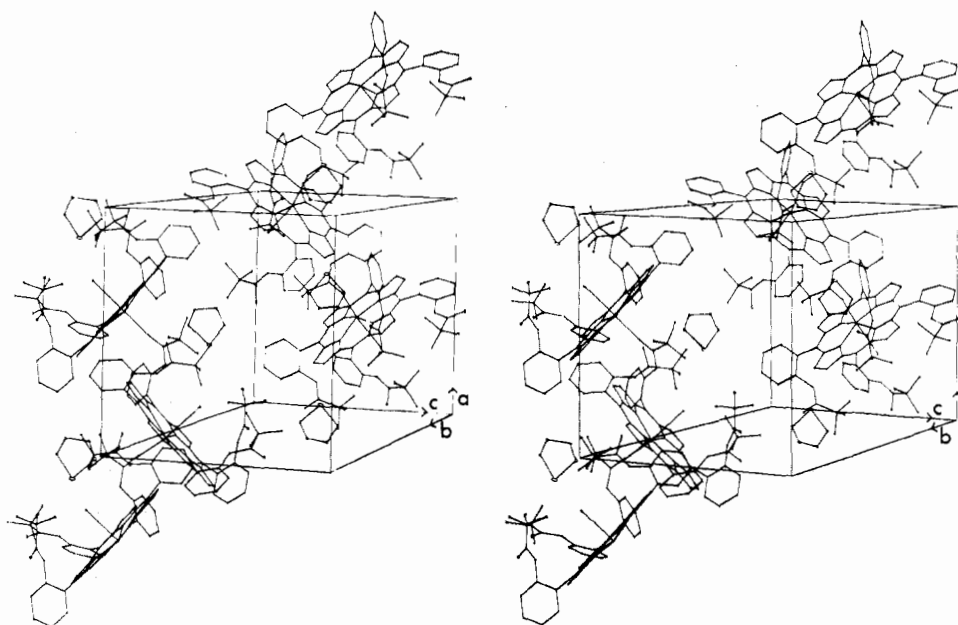


**Figure 3.** An ORTEP stereodiagram of the contents of the unit cell for polymeric Fe(TpivPP)(THT). Two extra Fe(TpivPP) units are shown to clarify packing.

**Table IV.** Bond Angles<sup>a</sup>

Atoms	Angle	Average	Atoms	Angle	Average	Atoms	Angle	Average
N(10)-Fe-N(30)	88.8 (5)		C(32)-C(33)-C(34)	107.7 (15)		N(51)-C(62)-O(50)	115 (3)	
N(10)-Fe-N(70)	89.3 (5)		C(51)-C(52)-C(53)	102.4 (17)		N(71)-C(82)-O(70)	117 (2)	118 (4)
N(30)-Fe-N(50)	88.8 (5)		C(52)-C(53)-C(54)	110.8 (17)		N(11)-C(22)-C(23)	121 (2)	
N(50)-Fe-N(70)	88.9 (5)	89.0 (2)	C(71)-C(72)-C(73)	107.1 (17)		N(31)-C(42)-C(43)	118.7 (19)	
N(10)-Fe-N(50)	164.0 (5)		C(72)-C(73)-C(74)	108.2 (16)	106.7 (34)	N(51)-C(62)-C(63)	131 (2)	
N(30)-Fe-N(70)	164.5 (6)	164.3	C(14)-C(15)-C(16)	116.4		N(71)-C(82)-C(83)	120.5 (17)	123 (6)
N(10)-Fe-O(1)	82.9 (6)		C(31)-C(15)-C(16)	117.2		O(10)-C(22)-C(23)	122 (3)	
N(30)-Fe-O(1)	83.6 (5)		C(34)-C(35)-C(36)	116.1		O(30)-C(42)-C(43)	117.4 (17)	
N(50)-Fe-O(1)	81.1 (6)		C(51)-C(35)-C(36)	119.6		O(50)-C(62)-C(63)	112 (3)	
N(70)-Fe-O(1)	81.0 (6)	82.2 (13)	C(54)-C(55)-C(56)	118.2		O(70)-C(82)-C(83)	122 (2)	118 (5)
N(10)-Fe-O(30')	93.3 (5)		C(71)-C(55)-C(56)	115.6		C(22)-C(23)-C(24)	111 (2)	
N(30)-Fe-O(30')	101.6 (5)		C(74)-C(75)-C(76)	115.2		C(22)-C(23)-C(25)	110 (2)	
N(50)-Fe-O(30')	102.7 (5)		C(11)-C(75)-C(76)	120.1	117.3 (18)	C(22)-C(23)-C(26)	109 (2)	
N(70)-Fe-O(30')	93.8 (5)	98 (5)	C(14)-C(15)-C(31)	126.2 (14)		C(24)-C(23)-C(25)	104 (2)	
O(1)-Fe-O(30')	173.6 (6)		C(34)-C(35)-C(51)	124.2 (15)		C(24)-C(23)-C(26)	110 (2)	
Fe-O(30')-C(42)'	160.3 (13)		C(54)-C(55)-C(71)	126.2 (17)		C(25)-C(23)-C(26)	113 (2)	
Fe-N(10)-C(11)	125.5 (11)		C(74)-C(75)-C(11)	124.5 (15)	125.3 (11)	C(42)-C(43)-C(44)	108.5 (17)	
Fe-N(10)-C(14)	128.1 (11)		C(15)-C(16)-C(17)	120.0		C(42)-C(43)-C(45)	106.8 (16)	
Fe-N(30)-C(31)	126.5 (10)		C(15)-C(16)-C(21)	119.9		C(42)-C(43)-C(46)	109.4 (16)	
Fe-N(30)-C(34)	127.2 (11)		C(35)-C(36)-C(37)	119.8		C(44)-C(43)-C(45)	108.7 (18)	
Fe-N(50)-C(51)	125.0 (12)		C(35)-C(36)-C(41)	119.8		C(44)-C(43)-C(46)	114.9 (17)	
Fe-N(50)-C(54)	126.0 (12)		C(55)-C(56)-C(57)	119.7		C(45)-C(43)-C(46)	108.2 (18)	
Fe-N(70)-C(71)	125.3 (12)		C(55)-C(56)-C(61)	120.2		C(62)-C(63)-C(64)	105 (2)	
Fe-N(70)-C(74)	126.2 (11)	126.2 (10)	C(75)-C(76)-C(77)	120.7		C(62)-C(63)-C(65)	107 (2)	
C(11)-N(10)-C(14)	105.7 (12)		C(75)-C(76)-C(81)	119.2		C(62)-C(63)-C(66)	117 (3)	
C(31)-N(30)-C(34)	106.1 (13)		N(11)-C(21)-C(20)	121.6		C(64)-C(63)-C(65)	109 (2)	
C(51)-N(50)-C(54)	108.6 (14)		N(11)-C(21)-C(16)	118.4		C(64)-C(63)-C(66)	107 (2)	
C(71)-N(70)-C(74)	108.1 (14)	107.1 (14)	N(31)-C(41)-C(40)	120.6		C(65)-C(63)-C(66)	111 (2)	
N(10)-C(11)-C(12)	109.0 (15)		N(31)-C(41)-C(36)	119.1		C(82)-C(83)-C(84)	108.0 (17)	
N(10)-C(14)-C(13)	111.8 (15)		N(51)-C(61)-C(60)	125.1		C(82)-C(83)-C(85)	107.0 (17)	
N(30)-C(31)-C(32)	111.8 (14)		N(51)-C(61)-C(56)	114.9		C(82)-C(83)-C(86)	104.1 (16)	
N(30)-C(34)-C(33)	110.1 (15)		N(71)-C(81)-C(80)	122.5		C(84)-C(83)-C(85)	114.8 (20)	
N(50)-C(51)-C(52)	110.7 (16)		N(71)-C(81)-C(76)	117.3		C(84)-C(83)-C(86)	111.8 (16)	
N(50)-C(54)-C(53)	107.6 (15)		C(21)-N(11)-C(22)	127.1		C(85)-C(83)-C(86)	110.5 (18)	109.4 (33)
N(70)-C(71)-C(72)	109.6 (17)		C(41)-N(31)-C(42)	126.3		C(1)-S-C(4)	86.9 (17)	
N(70)-C(74)-C(73)	107.0 (15)	109.7 (18)	C(61)-N(51)-C(62)	137.2		S-C(1)-C(2)	108 (4)	
C(11)-C(12)-C(13)	110.9 (17)		C(81)-N(71)-C(82)	132.1	130 (5)	S-C(4)-C(3)	108 (4)	
C(12)-C(13)-C(14)	102.5 (16)		N(11)-C(22)-O(10)	117 (3)		C(1)-C(2)-C(3)	118 (5)	
C(31)-C(32)-C(33)	104.2 (14)		N(31)-C(42)-O(30)	124 (2)		C(2)-C(3)-C(4)	114 (4)	

<sup>a</sup> See footnote, Table III.

obtuse than the expected angle of 120° for an sp<sup>2</sup>-hybridized pivalamide oxygen atom.

Bond lengths around the metal center are typical of high-spin metalloporphyrins with occupied metal 3d<sub>z<sup>2</sup></sub> and

3d<sub>x<sup>2</sup>-y<sup>2</sup></sub> orbitals. Long axial bond lengths, Fe-L<sub>ax</sub>, and N<sub>porph</sub>...L<sub>ax</sub> separations close to the sum of the van der Waals radii of the atoms are typical of a (3d<sub>z<sup>2</sup></sub>)<sup>2</sup> configuration.<sup>2</sup> The O(30')...N<sub>porph</sub> separations are in the range 3.11 (2)-3.36 (2)

Table V. Inter Fe(TpivPP) Unit Contacts (&lt;3.75 Å)

Fe-C(42) <sup>a</sup>	3.420 (20)	C(35)-C(44)'	3.63 (3)
S-C(26)	4.08 (3)	N(30)-C(44)'	3.72 (2)
S-N(31)	4.10 (3)	C(34)-C(44)'	3.57 (3)
S-C(78)	3.87	N(50)-C(45)'	3.57 (3)
C(1)-O(10)	3.53 (4)	C(54)-C(45)'	3.69 (3)
C(2)-C(45)	3.71 (5)	C(72)-O(10)	3.65 (3)
C(3)-O(50)	3.32 (5)	C(73)-O(10)	3.30 (3)
C(4)-O(50)	3.48 (5)	C(45)-O(70)	3.73 (3)
O(1)-Fe	2.897 (19)	C(46)-O(70)	3.50 (3)
O(1)-C(25)	2.94 (3)	C(53)-C(17)	3.49
O(1)-C(64)	3.05 (4)	C(72)-C(20)	3.74
O(1)-N(70)	3.29 (12)	O(50)-C(37)'	3.38
O(30)-N(10)	3.107 (19)	O(50)-C(38)'	3.29
O(30)-N(20)	3.139 (19)	C(39)-C(77)'	3.72
O(30)-N(30)	3.328 (18)	C(40)-C(11)'	3.69
O(30)-N(50)	3.362 (19)	C(2)-C(57)	3.61
O(30)-C(52)	3.61 (2)	C(65)-C(58)	3.64
O(1)-N(50)	3.29 (2)	C(32)-C(58)'	3.73
O(1)-N(10)	3.34 (3)	C(59)-C(80)	3.72
O(1)-N(30)	3.37 (2)	C(32)-C(59)'	3.72
O(1)-C(85)	3.49 (2)	C(59)-C(79)	3.74

<sup>a</sup> Primed atoms belong to the same polymeric chain as the unprimed atoms.

Å and the O(1)⋯N<sub>porph</sub> separations are in the range 3.29 (2)–to 3.37 (2) Å. Ignoring for the moment the semicoordinated water molecule, the Fe–O(30)' separation is comparable with the Fe–N<sub>imid</sub> separation of 2.161 (5) Å observed for the pure five-coordinate complex Fe(TPP)(2-Me-imid).<sup>2</sup> The Fe–N<sub>porph</sub> and Ct⋯N<sub>porph</sub> separations for these two complexes are quite similar; both are high-spin (*S* = 2) iron(II) species.

The substantial out-of-plane displacement of the iron center, may be correlated with the (3d<sub>x<sup>2</sup>-y<sup>2</sup>)<sup>2</sup> configuration. The 0.28 Å displacement observed here and the 0.42 Å displacement observed for Fe(TPP)(2-Me-imid)<sup>2</sup> may be compared with the displacements of 0.09 and 0.13 Å observed for the six-coordinate complex Mn<sup>III</sup>(TPP)(N<sub>3</sub>)(HOCH<sub>3</sub>)<sup>13</sup> and the five-coordinate complex Co<sup>II</sup>(TPP)(1-Me-imid),<sup>14</sup> respectively; these latter two complexes have a vacant 3d<sub>x<sup>2</sup>-y<sup>2</sup> orbital.</sub></sub>

### Discussion of the "Picket Fence" Porphyrin Structures

The structures of three iron(II) "picket fence" porphyrin derivatives have now been determined in this laboratory,<sup>11,15</sup> and in all cases crystal twinning and poor mosaicity, poorly defined solvate species, and high thermal motion of the pivalamide "pickets" have been encountered.

The TpivPP moiety does not maintain an invariant conformation. In polymeric Fe(TpivPP) the amide groups (e.g., Piv-11 = N(11), C(22), O(10), C(23)) are not coplanar with their attached phenyl group; the dihedral angles are 41.6, 43.2, 19.8, and 168.9° for Piv-11 to Piv-76, respectively. For Fe(TpivPP)(1-Me-imid)(O<sub>2</sub>) the departures from coplanarity are smaller; the dihedral angles are approximately 5 and 17°. The amide groups themselves are approximately planar. Furthermore the dihedral angles between the porphinato plane and phenyl groups phenyl-16 to phenyl-76 are, respectively, 73.6, 65.9, 108.1, and 115.0° for polymeric Fe(TpivPP), but for Fe(TpivPP)(1-Me-imid)(O<sub>2</sub>) the relevant angles are 102.1 and 83.2°, and for Fe(TpivPP)(THT)(O<sub>2</sub>) 106.3, 97.7, 80.6, and 73.4°.

These two conformational features can be correlated with the "depth" of the protected pocket created by the pivalamidephenyl "pickets". This is defined as the mean distance of the pivalamide methyl carbon atoms from the porphinato plane. For polymeric Fe(TpivPP) the depth is 4.69 Å, for Fe(TpivPP)(1-Me-imid)(O<sub>2</sub>) 5.05 Å, and for Fe(TpivPP)(THT)(O<sub>2</sub>) 5.01 Å.

In Fe(TpivPP)(1-Me-imid)(O<sub>2</sub>)<sup>11</sup> the porphinato core is ruffled in quasi-*D*<sub>2d</sub> fashion. Moreover, the angles between vectors of the type C(16)⋯C(19) and the normal to the

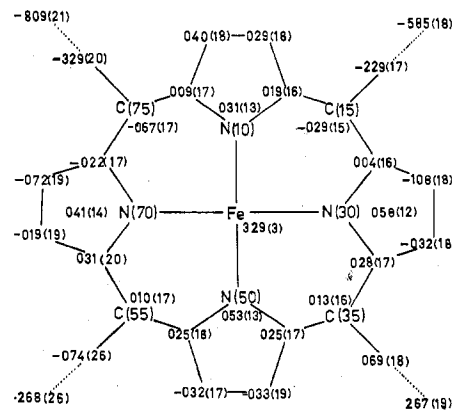


Figure 4. Displacements of atoms from the least-squares plane of the 24-atom porphinato skeleton for polymeric Fe(TpivPP)(THT).

porphinato plane are such that the pivalamidophenyl "pickets" can be viewed as leaning "outward". For Fe(TpivPP)(THT)(O<sub>2</sub>)<sup>15</sup> three pickets lean outward and the fourth leans inward, but for polymeric Fe(TpivPP) the opposite is observed. In this latter case the leaning inward can be associated with the doming of the porphinato core. In both of these complexes the orientation of the pyrrole groups does not follow a simple symmetrical pattern. The displacements of atoms from the least-squares plane of the 24-atom porphinato skeleton for polymeric Fe(TpivPP) are illustrated in Figure 4.

Novel features of polymeric [Fe(TpivPP)(OH<sub>2</sub>)]·THT, in relation to other five- or six-coordinate metal(II) porphinato derivatives, include no nitrogen axial ligand, coordination of an amide oxygen atom, and semicoordination of a water molecule.

**Acknowledgment.** This work was supported in part by National Science Foundation Grant CHE75-17018 and National Institutes of Health Grant GM-17880 and by the Medical Research Council of New Zealand. The authors also gratefully acknowledge the Universities Grants Committee for equipment and for a Shirtcliffe Fellowship and a Postgraduate Scholarship (G.B.J.).

**Registry No.** [Fe(TpivPP)(OH<sub>2</sub>)]·THT, 65071-47-8.

**Supplementary Material Available:** A listing of structure factor amplitudes (13 pages). Ordering information is given on any current masthead page.

### References and Notes

- (1) University of Canterbury. (b) Stanford University.
- (2) J. L. Hoard in "Porphyrins and Metalloporphyrins", K. M. Smith, Ed., Elsevier, Amsterdam, 1975, pp 317–380.
- (3) Abbreviations: TpivPP, *meso*-tetrakis(α,α,α,α-o-pivalamidophenyl)-porphinato; TPP, *meso*-tetraphenylporphinato; THT, tetrahydrothiophene; 1-Me-imid, 1-methylimidazole; 2-Me-imid, 2-methylimidazole; acac, acetylacetonate.
- (4) (a) I. C. Gunsalus, J. R. Meeks, J. D. Lipscomb, P. Debrunner, and E. Munk in "Molecular Mechanisms of Oxygen Activation", O. Hayaishi, Ed., Academic Press, New York, N.Y., 1973, Chapter 14. (b) C. A. Tyson, J. D. Lipscomb, and I. C. Gunsalus, *J. Biol. Chem.*, **247**, 5777 (1972).
- (5) C. K. Chang and D. Dolphin, *J. Am. Chem. Soc.*, **98**, 1607 (1976).
- (6) (a) S. C. Tang, S. Koch, G. C. Papaefthymiou, S. Foner, R. B. Frankel, J. A. Ibers, and R. H. Holm, *J. Am. Chem. Soc.*, **98**, 2414 (1976); (b) S. Koch, S. C. Tang, R. H. Holm, and R. B. Frankel, *ibid.*, **97**, 914 (1975); (c) S. Koch, S. C. Tang, R. H. Holm, R. B. Frankel, and J. A. Ibers, *ibid.*, **97**, 916 (1975); (d) J. P. Collman, T. N. Sorrell, and B. M. Hoffman, *ibid.*, **97**, 913 (1975); (e) J. P. Collman and T. N. Sorrell, *ibid.*, **97**, 4135 (1975); (f) J. P. Collman, T. N. Sorrell, J. D. Dawson, J. R. Trudell, E. Bunnenberg, and C. Djerassi, *Proc. Natl. Acad. Sci. U.S.A.*, **73**, 6 (1976); (g) C. K. Chang and D. Dolphin, *J. Am. Chem. Soc.*, **97**, 5948 (1975).
- (7) L. R. Ocone and B. P. Block, *Inorg. Synth.*, 125 (1966).
- (8) J. P. Collman, R. R. Gagne, C. A. Reed, T. R. Halbert, G. Lang, and W. T. Robinson, *J. Am. Chem. Soc.*, **97**, 1427 (1975).
- (9) K. Spartalian, G. Lang, J. P. Collman, R. R. Gagne, and C. A. Reed, *J. Chem. Phys.*, **63**, 5375 (1975).
- (10) "International Tables for X-Ray Crystallography", Vol I, Kynoch Press, Birmingham, England, 1962.

- (11) G. B. Jameson, G. A. Rodley, W. T. Robinson, R. R. Gagne, C. A. Reed, and J. P. Collman, *Inorg. Chem.*, preceding paper in this issue.
- (12) Reflections with  $|F_o| < 0.25 |F_c|$  or  $|F_o| > 4 |F_c|$  were not included in the synthesis.
- (13) V. W. Day, B. R. Stults, E. L. Tasset, R. D. Day, and R. S. Marianelli, *J. Am. Chem. Soc.*, **96**, 2650 (1974).
- (14) W. R. Scheidt, *J. Am. Chem. Soc.*, **96**, 90 (1974).
- (15) The crystal structure of the dioxygen adduct of  $[\text{Fe}(\text{TpivPP})\text{-(THT)}]_2\text{(THT)}$  has also been determined. Crystal and refinement data:

monoclinic;  $P2_1/c$ ;  $Z = 4$ ;  $a = 16.951$  (3),  $b = 18.153$  (4),  $c = 25.470$  (4) Å;  $\beta = 107.14$  (8)°;  $R = 0.17$ ,  $R_w = 0.15$  for 1521 reflections having  $I > \sigma_I$ . The best data obtainable were severely limited in extent ( $2\theta_{\text{max}} = 29.2^\circ$ ) and quality, and the resultant structure analysis is therefore only semiquantitative. Dioxygen adopts the end-on bent bond mode of coordination found for  $\text{Fe}(\text{TpivPP})(1\text{-Me-imid})(\text{O}_2)$ ; the Fe-S separation is 2.49 (2) Å, the Fe-N<sub>porph</sub> separations are in the range of 1.99–2.00 Å, and the dihedral angle between the least-squares planes of the porphinato skeleton and THT axial base is 44°.

Contribution from the Center for Molecular Structure, Department of Chemistry, University of Florida, Gainesville, Florida 32611

## Pentagonal-Bipyramidal Complexes. Crystal and Molecular Structures of Chloroaqua(2,6-diacetylpyridine bis(semicarbazone))manganese(II), -iron(II), -cobalt(II), and -zinc(II) Chloride Dihydrates

GUS J. PALENIK\* and DENNIS W. WESTER<sup>1</sup>

Received October 14, 1977

The complexes  $[\text{M}(\text{DAPSC})(\text{Cl})(\text{H}_2\text{O})]^+\text{Cl}^- \cdot 2\text{H}_2\text{O}$ , where M = Mn, Fe, Co, or Zn and DAPSC is 2,6-diacetylpyridine bis(semicarbazone), are isomorphous. The space group is *Ia* and there are four molecules per unit cell. The cell dimensions are  $a = 18.322$  (3), 18.096 (2), 17.968 (3), and 18.038 (11);  $b = 13.076$  (5), 13.111 (4), 13.139 (8), and 13.112 (5); and  $c = 8.128$  (1), 8.061 (1), 8.052 (2), and 8.066 (3) Å, with  $\beta = 99.98$  (1), 99.76 (1), 99.86 (2), and 100.28 (4)°, for the Mn, Fe, Co, and Zn complexes, respectively. The structures were solved by the heavy-atom method and refined by least-squares techniques to final unweighted *R* values of 0.039, 0.040, 0.039, and 0.058 for the Mn, Fe, Co, and Zn complexes. The cation  $[\text{M}(\text{DAPSC})(\text{Cl})(\text{H}_2\text{O})]^+$  is a pentagonal bipyramid with the metal ion in the center. The Cl and H<sub>2</sub>O groups are axial, with the planar pentadentate ligand DAPSC forming the equatorial plane. An unusual feature of this series is the decrease in the axial M–Cl and M–OH<sub>2</sub> distances from Mn to Zn without the expected break. However, the M–equatorial donor distances increase from Co to Zn as predicted from the splitting pattern of the d orbitals in a pentagonal-bipyramidal field. This observation is discussed in terms of the nonbonded interactions between the axial and equatorial groups. A comparison of the dimensions of the  $[\text{M}(\text{DAPSC})(\text{Cl})(\text{H}_2\text{O})]^+$  ions with other seven-coordinate complexes is given.

### Introduction

Seven-coordinate complexes of the elements scandium to zinc are relatively rare. The first, well-characterized, seven-coordinate species were the anionic ethylenediaminetetraacetato (EDTA) complexes of Mn(II)<sup>2</sup> and Fe(III)<sup>3</sup> and the *trans*-1,2-diaminocyclohexane-*N,N'*-tetraacetato (DCTA) complex of Fe(III).<sup>4</sup> In these three complexes the hexadentate ligand and a water molecule are coordinated to the central metal ion at the vertices of a somewhat irregular polyhedron.<sup>5</sup> Next, pentagonal-bipyramidal complexes of Fe(III) were synthesized using a pentadentate macrocycle<sup>6</sup> and were characterized by x-ray diffraction techniques.<sup>7</sup> In the above Mn(II) and Fe(III) complexes the metal ions are high-spin d<sup>5</sup> species which are spherically symmetric. Therefore, there is no crystal field stabilization for any particular geometry. The first, seven-coordinate complex with a nonspherical first-row transition-metal ion was a Ti(III) species<sup>8</sup> which was followed by a preliminary report on the pentagonal-bipyramidal V(CN)<sub>7</sub><sup>−4</sup> ion.<sup>9a</sup>

Previously, however, there has been no systematic investigation in which ligands were designed to produce seven-coordinate complexes consistently. Our earlier studies with thiosemicarbazones<sup>10</sup> and semicarbazones<sup>11</sup> suggested that 2,6-diacetylpyridine bis(semicarbazone), henceforth DAPSC, would be ideally suited to forming pentagonal-bipyramidal complexes with a variety of different metal ions. Indeed, the  $(\text{M}(\text{DAPSC})(\text{H}_2\text{O})(\text{Cl}))^+\text{Cl}^- \cdot 2\text{H}_2\text{O}$ , M = Mn, Fe, Co, and Zn, complexes were found to be isomorphous and all contained a pentagonal-bipyramidal cation.<sup>12</sup> The crystal structure of these complexes is presented in this report with the synthesis and characterization to be presented later.<sup>13</sup> Following our preliminary report,<sup>12</sup> seven-coordinate complexes of Ti(IV),<sup>14</sup>

Mn(II),<sup>15–17</sup> Fe(II),<sup>18,19</sup> Fe(III),<sup>20</sup> Co(II),<sup>21</sup> and Zn(II)<sup>22</sup> have been reported. In addition, our own studies with DAPSC have yielded pentagonal-bipyramidal complexes of Ni(II),<sup>23</sup> Cu(II),<sup>23</sup> Cr(III),<sup>24</sup> Fe(III),<sup>24</sup> and Sc(III).<sup>25</sup> A related planar pentadentate ligand, 2,6-diacetylpyridine bis(2'-pyridylhydrazone), has produced pentagonal-bipyramidal complexes with Co(II)<sup>26</sup> and Zn(II).<sup>26</sup>

### Experimental Section

**Data Collection and Reduction.** Preliminary precession photographs were taken of all four complexes. The photographs indicated that the four compounds were isomorphous. The crystals are monoclinic with the space groups *Ia* or *I2/a* as deduced from the systematic absences ( $h + k + l = 2n + 1$  and  $h0l$  if  $h = 2n + 1$ ). In each case a second crystal was used to measure the intensity data with a Syntex P1 diffractometer. The pertinent crystal data together with other details of the intensity measurements are given in Table I. A variable speed (1–24°/min)  $\theta$ – $2\theta$  scan technique was used in measuring the intensity. A set of 4 standard reflections was measured after every 96 measurements and was used to correct for a small change in the intensities of the standards with time. In the Mn case the standards decreased by about 10% over the period of data collection, but the other three complexes showed variations of less than ±3%. Reflections with an intensity  $I \geq k\sigma(I)$ , see Table I for the various *k* values, were considered reliable and were used in the analysis. The remaining reflections were flagged with a minus sign and were not used in the structure determination or refinement. No absorption corrections were made because of the small size of the crystals and the small value of  $\mu$ .

**Structure Determination and Refinement.** The structure of the zinc complex was determined first. The intensity distribution for all four complexes was midway between the centric and acentric cases, suggesting that the correct space group was *Ia*. The *y* coordinate for the zinc atom was determined from the Patterson function, and the *x* and *y* coordinates were chosen to be  $1/4$ . The Fourier synthesis based